Automated in-process cure monitoring of composite laminates using a guided wave-based system with high temperature piezoelectric transducers

Tyler B. Hudson[1,2*] and Fuh-Gwo Yuan[1,2]

[1] North Carolina State University, Department of Mechanical and Aerospace Engineering, 911 Oval Drive - 3306 EBIII, Campus Box 7910, Raleigh, NC 27695, United States

[2] National Institute of Aerospace, 100 Exploration Way, Hampton, VA 23666, United States

*Corresponding Author: tyler.b.hudson@nasa.gov

Keywords: *Cure monitoring, Guided waves, Piezoelectric transducers, Composites, Gelation, Vitrification, Hilbert transform.*

A guided wave-based in-process cure monitoring technique for carbon fiber reinforced polymer (CFRP) composites was investigated. Key transition points during the cure cycle (e.g., minimum viscosity, gelation, and vitrification) were identified experimentally using the amplitude and group velocity of guided waves, and validated using the commercial-off-the-shelf cure process modeling software RAVEN®. Using the automated system, high-temperature piezoelectric transducers were utilized to interrogate a twenty-four ply unidirectional composite panel fabricated from Hexcel® IM7/8552 prepreg during cure in an oven. First, as the resin melted and the composite consolidated, an increase in the normalized peak voltage of the guided waves was observed. During the ramp to 177°C, the viscosity dropped to a minimum and this corresponded to the maximum normalized peak voltage. When the resin began to gel, the normalized amplitude started dropping and continued to drop throughout gelation. Lastly, the normalized peak voltage increased through vitrification (transition from rubbery to glassy state) before nearing a plateau close to the end of cure. Also during the transition from rubbery to glassy state, as the degree of cure simulated by RAVEN® increased, the group velocity of the guided waves increased (i.e., degree of cure was directly proportional to group velocity). This work demonstrated the feasibility of in-process cure monitoring as well as continued progress toward defect detection during cure, and ultimately a closed-loop process control to maximize composite part quality and consistency.

1. Introduction

In the polymer composites industry, cure cycles for composite parts are typically developed from a "trial and error" or a more effective "processing science" approach to reduce the final porosity level in the composite laminate [1]. Porosity [2] is defined as "large number of microvoids … which collectively may reduce the mechanical properties of the components to an unacceptable degree," but "each of which is too small to be of structural significance or to be detected individually by a realistic inspection technique." Typically, porosity occurs because of entrapped air, moisture, or volatile products during the curing cycle [2]. Although this work does not address

the issue of porosity directly, an automated guided wave-based system is under development to perform cure monitoring with the future goal of defect detection during cure.

Several cure monitoring techniques currently exist, each having its own merits and challenges. Differential scanning calorimetry (DSC), rheology, dynamic mechanical analysis (DMA), and thermal gravimetric analysis (TGA) are methods to characterize the thermo-physical and mechanical properties of a resin during cure, but must be conducted on a small sample in a controlled lab instrument. Therefore, these methods cannot be used for in-process cure monitoring.

DSC has been applied to study the curing of epoxy resins for decades [3-7]. DSC is primarily used to observe phase transitions including the melting point and the glass transition temperature (T_g) as well as heat of reaction to measure degree of cure (DOC) before or after a cure cycle has been applied. This lab-scale test utilizes a several milligram sample.

Another well-established, laboratory-scale (approximately 1 gram sample) technique for material characterization is rheology. Rheology is generally conducted when the sample is in the liquid state. A rheometer can measure the viscosity, shear storage modulus, G', which is a measure of the sample's elastic properties, and shear loss modulus, G'', which is a measure of the sample's viscous properties. The metric tan δ (tan $\delta = G''/ G'$) is often reported as well. Epoxy resins have been studied by rheology for over 50 years [8-10]. Similar to rheology, DMA determines the viscoelastic properties of a material by applying a sinusoidal stress and measuring the strain in the material. DMA investigates the longitudinal moduli, E' and E'', and can be used to identify T_g as well as transitions associated with molecular motions [11,12].

TGA most often is used to measure mass change (gain or loss) of a material due to loss of volatiles, oxidation, and/or decomposition/degradation as a function of temperature (constant heating rate) or time (constant temperature). This provides information on the physical and chemical properties of the material. It is used extensively on polymeric materials [13]. As stated previously, DSC, rheology, DMA, and TGA are all lab-scale, material characterization, baseline tests by which many proposed cure monitoring techniques have been compared.

Dielectric analysis (DEA) is an in-process cure monitoring technique that utilizes a loss factor, ε'', which has contributions from conductivity and dipole relaxation time, to monitor the different phases of cure (e.g., in glass-fiber reinforced epoxy [14]). The degree of cure measured from DEA correlates well with DSC and Raman spectroscopy for isothermal cure of in epoxy resins [7]. During the resin transfer molding process, the maximum of the ionic conductivity indicated minimum viscosity. After minimum viscosity occurs, the first zero slope of the derivative of log of the ionic conductivity with respect to the cure time (DLIC) demarks the onset of gelation. DLIC also loosely correlated with degree of cure after gelation to full cure and the DLIC plateau estimated vitrification when compared with DSC [12]. Although these tests were performed in a

laboratory environment, one of the primary advantages of DEA is the ability to implement in-situ cure monitoring at the production scale.

Fourier transform (FT)-infrared (IR) spectroscopy can be performed in-situ with fairly inexpensive uncoated optical fiber in many cure monitoring systems including thermosetting composites [15]. An FT-IR spectrometer, operating in the near infrared (NIR) range can monitor cure by tracking absorbance peaks in the spectral information. A decrease in epoxy absorbance, decrease in amine absorbance, and an increase in hydroxyl absorbance was observed during isothermal cure [16]. Fiber optic FT-Raman spectroscopy investigated the spectral information during cure of a high temperature (330°C) polymerization reaction. The progression of the reaction was identified by the intensity of the Raman shift. In addition, the spectral information was able to provide information about two different reactions. The primary advantages to this method are the ability to operate at high temperature, in-situ measurements (directly implemented into air oven), and real-time information [17,18]. Using the same system that can perform FT-Raman spectroscopy during cure, FT-NIR can investigate the chemical composition post-cure [19].

Conventional bulk wave ultrasound has also been implemented as a cure monitoring technique. In previous work with thermoset resins, ultrasonic velocity has been used to infer the degree of cure because of its association with the modulus of the resin [20-22]. Bulk wave ultrasound, in pulse-echo mode, can monitor the completion of resin cure based on when the time delay plateaus (i.e., the ultrasonic velocity stops increasing) in graphite/epoxy composites [23] and epoxy matrices [24]. Non-contact, air-coupled transducers can be used for ultrasonic velocity measurement in resins when line of sight is available during cure [25]. Mounting piezoceramic actuators and sensors on the mold can alleviate unreliable coupling between an ultrasound transducer and the mold which can occur during phases of heating and cooling [26]. Other ultrasonic phenomena have also been used for monitoring degree of cure including, attenuation (i.e., amplitude of signal) [2,22,23,27,28], instantaneous phase, and the "mean value of each frequency curve weighted by the maximum corresponding spectral amplitude" [29].

The guided wave system proposed in this work was designed to complement the current cure monitoring technologies. The guided wave system has the advantage of being in-situ incorporated directly into the standard curing equipment and technique. This system is not a stand-alone bench-top lab system where the material is tested outside its production environment (e.g., DSC, rheology, DMA, TGA). The system is scalable from producing flat composite panels to full-scale complex structures utilized in aerospace and space applications (e.g., cylinders/barrels, wing skins, etc.). The current system is composed of a robust linear array of high temperature piezoelectric transducers incorporating modifications identified during its development [30]. In the future, a linear array of high temperature piezoelectric transducers could be replaced by a single multiplexed optical fiber with phase-shifted fiber Bragg gratings (PS-FBGs) which can sense wave signals during cure and in-service, enabling life cycle monitoring as the sensors remain embedded in the composite.

The guided wave approach, unlike conventional ultrasound that only provides information about the part directly underneath or near the ultrasonic transducer, interrogates a continuous wave path through the thickness of the panel along the line from actuator to sensor. Using a guided wave approach in carbon fiber reinforced polymer (CFRP) laminates, it has been recently demonstrated that the group velocity of guided waves propagating in-plane, normal to the carbon fiber, increased as final degree of cure of the composite increased and the expected porosity level decreased [31]. However, this work was post cure on three separate composite panels. If key cure parameters (e.g., viscosity, degree of cure, T_g, gelation, vitrification, porosity), can be estimated during cure, the process parameters can be dynamically tuned based on the measurements. This would prevent the operator from having to strictly follow a non-optimized fixed cure cycle.

This work examined the amplitude and group velocity of guided waves in CFRP panels (Size: 610 mm × 178 mm) during cure in real-time. The feasibility of using these metrics to identify the key transition points during the cure cycle (e.g., minimum viscosity, gelation, and vitrification) and the state of the resin was investigated. The transformation of the resin from the liquid to rubbery state is typically referred to as gelation. The subsequent transformation from the rubbery state to the glass state is defined as vitrification [32]. A generalized time-temperature-transformation (TTT) diagram [33-35] for an epoxy matrix (e.g., Hexcel® 8552) with a two stage cure cycle (without ramp to first hold) is shown in Figure 1 denoting these phase transformations. In the figure, T_{g0} denotes the glass transition temperature of the initial formulation (completely uncured), $T_{g\infty}$ represents the glass transition temperature of the cross-linked resin at full cure [35], sol refers to solvent-soluble (i.e., ungelled), and gel refers to solvent-insoluble [33,34].

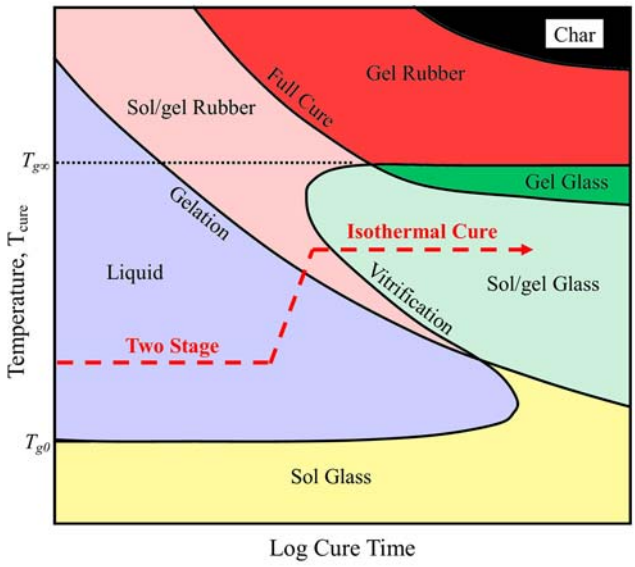

Figure 1. Generalized time-temperature-transformation (TTT) diagram for an epoxy matrix (e.g., T_{g0} = -7°C, and $T_{g\infty}$ = 250°C for Hexcel® 8552)

For comparison with experimental results, a semi-empirical cure process model was simulated with the specific cure parameters used in experiment. Part one of the modeling flow chart (Figure

2) illustrates the modeling procedure used to validate phase transitions (gelation, vitrification) and physical parameters from simulation using waveguide-based measurements. Part two describes future work to be performed by the group to compare the group velocity between the proposed waveguide system and simulation predictions based on mechanical properties.

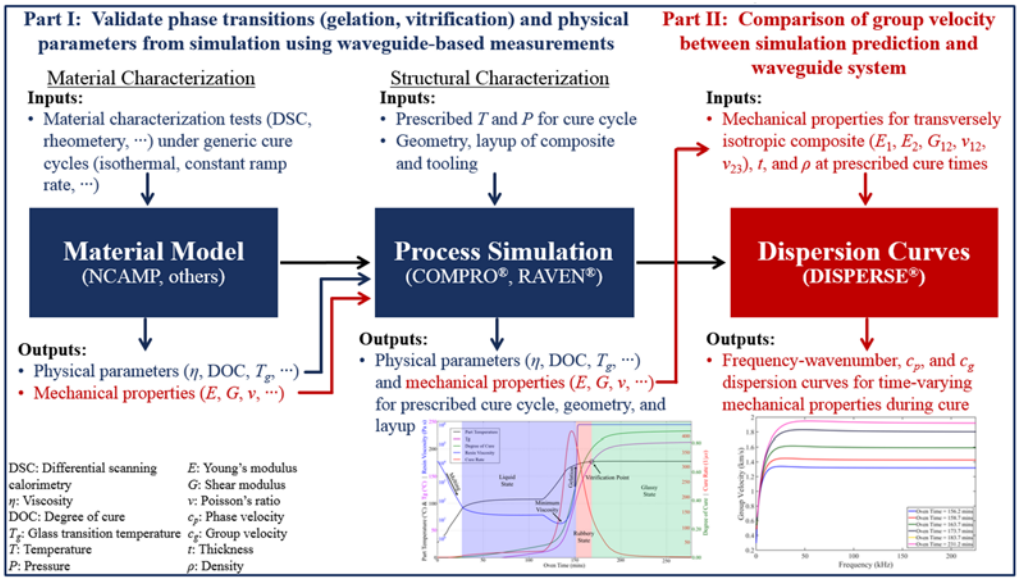

Figure 2. Modeling flow chart for composite cure process simulation to compare with experimental waveguide-based measurements.

2. Materials and Methods

Two twenty-four ply panels were laid up by hand using IM7/8552, 35% RC, 190 gsm unidirectional prepreg (Hexcel® Corporation). The panels were 610 mm × 178 mm × 4.6 mm (nominal) and the layup was $[0_{24}]$. The panels were cured in an oven (Figure 3) following two commonly used cure cycles for this material system. The first cure cycle was a two stage cure with a B-stage hold. The temperature was ramped to 107°C at 2.8°C/min, held one hour, ramped to 177°C at 2.8°C/min, held two hours, then cooled down. The second cure cycle, commonly used in industry for thin laminates to save time, energy, and thus money removed the B-stage (107°C) hold and ramped directly to 177°C at 2.8°C/min, held two hours, then cooled down. Both panels were interrogated during the entire cure period through guided waves. A guided wave was excited into the plate using a five-cycle Hanning windowed sinusoidal toneburst signal emitted from a waveform generator (Agilent Technologies: 81150A) to an amplifier (Krohn-Hite Corporation: Model 7602M) to a piezoelectric transducer [Physical Acoustics Corporation: Nano-30 (⌀7.9 mm, height 7.1 mm)] that was rated for use up to 177°C. The amplifier magnified the input signal to a peak-to-peak voltage of approximately 120 V. The plate response along the fiber direction was recorded by identical piezoelectric transducers in a pitch-catch configuration on two oscilloscopes (Agilent Technologies: MSO9064A and Tektronix: MSO3014). Instrumentation shown in Figure 3.

Fluorinated ethylene propylene (FEP) release film was placed on the top and bottom of the composite panel. The sensors were bonded to a thin (0.1 mm) sheet of steel ("caul" plate) that was placed on top of the panel which prevented the sensors from being pressed into the panel during cure while still allowing the guided wave in the composite to be measured. The sensors (1-8) were located at a distance, x, from the actuator of 57, 76, 95, 114, 133, 152, 171, and 190 mm, respectively. A breather cloth and vacuum bag covered the panel and full vacuum was applied using a vacuum pump (Figure 3). An oven was used to cure the panel as part of the building-block approach to developing the guided wave system for use in an autoclave where the recommended 690 kPa pressure can be used. By following this approach, the port in the back of the oven could be utilized for the ingress/egress of all cables during development of the system prior to making modifications to the autoclave. It should be noted that the goal of the current work was not to produce a high quality composite panel but rather to develop and test the guided wave system at elevated temperatures during cure and determine what meaningful information can be derived from the results.

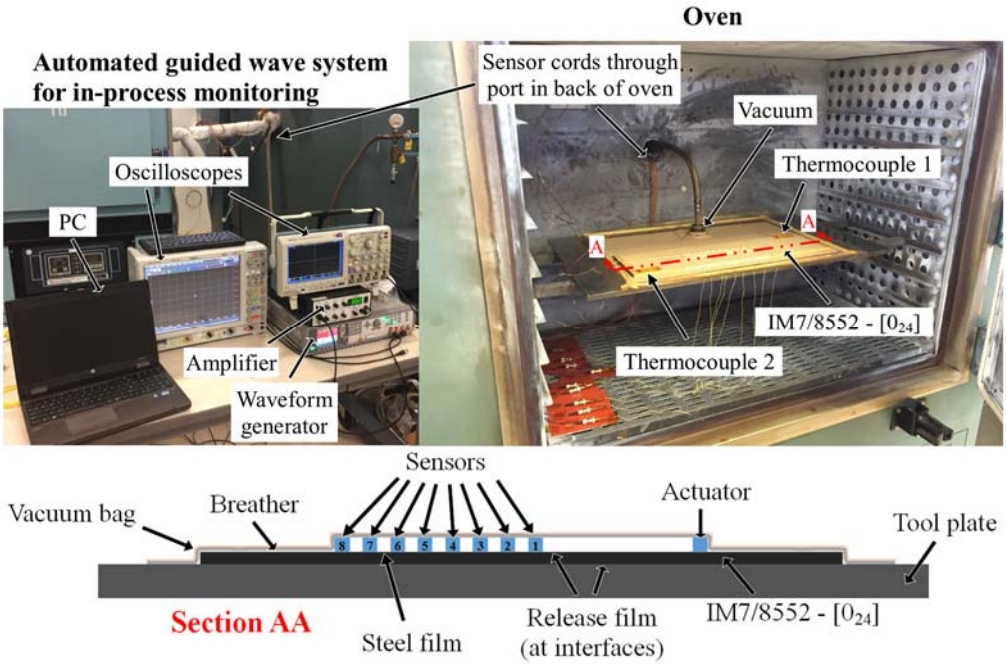

Figure 3. An automated guided wave system for in-process cure monitoring.

The automation code for the sensing system was written in MatLab® and utilized the Instrument Control Toolbox to control both the waveform generator and the oscilloscopes. The general procedure of the algorithm is outlined in Figure 4. The center frequency of the five-cycle, Hanning windowed sinusoidal toneburst signal was set on the waveform generator. During each iteration, the center frequency was cycled through fourteen frequencies (100, 110, 120, 130, 140, 150, 160, 175, 200, 225, 250, 275, 300, 325, and 350 kHz). The range of voltages to be measured by the oscilloscope was set based on the peak voltage recorded at that center frequency on the previous iteration. Dynamically scaling the range on the oscilloscope based on the previous iteration

ensured that the range was minimized to increase signal to noise ratio (SNR) while keeping it large enough to prevent the recorded voltage from being cut off. After the equipment was set, sixteen measurements were averaged on the oscilloscope and transferred to the computer. These data were processed through a bandpass filter and analyzed in real-time using MatLab®. The instantaneous recorded waveforms, the full time history waveforms, and key metrics such as peak voltage were all displayed on-screen during cure. This process was iterated throughout the cure of the part.

Figure 4. Automated algorithm for data collection and analysis of guided waves for in-process cure monitoring.

3. Results

The plate response at sensor 4 (Figure 3) for five-cycle Hanning window toneburst actuation with center frequency 140 kHz at cure time around 270 minutes in the entire cure cycle is shown in Figure 5.

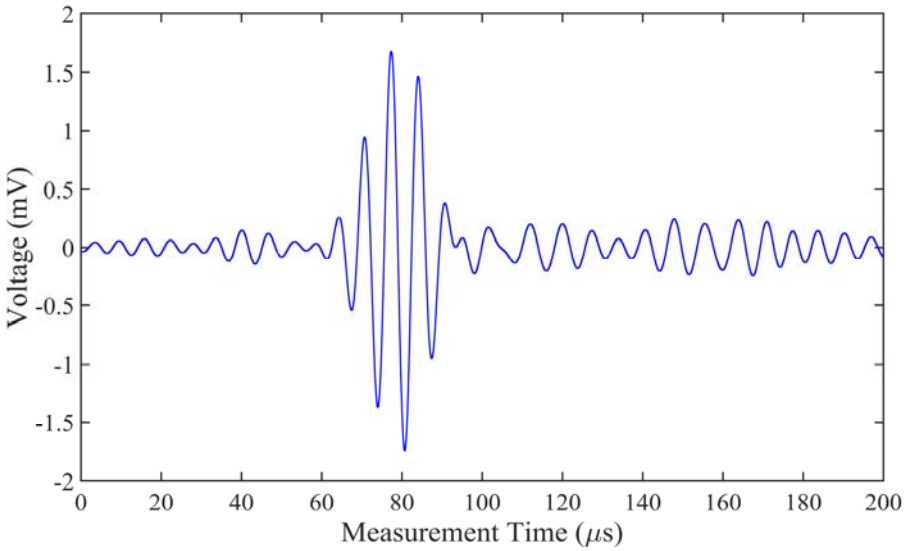

Figure 5. Plate response at Sensor 4 for five-cycle Hanning window toneburst actuation with center frequency 140 kHz at oven time 272 minutes.

By assembling each individual waveform data at a particular sensor and center frequency of actuation, the full time history of the plate response can be viewed as a three-dimensional surface and contour plot. This is shown for sensor 4 with an actuation center frequency of 140 kHz in Figure 6. Figure 5 is the last "slice" of Figure 6.

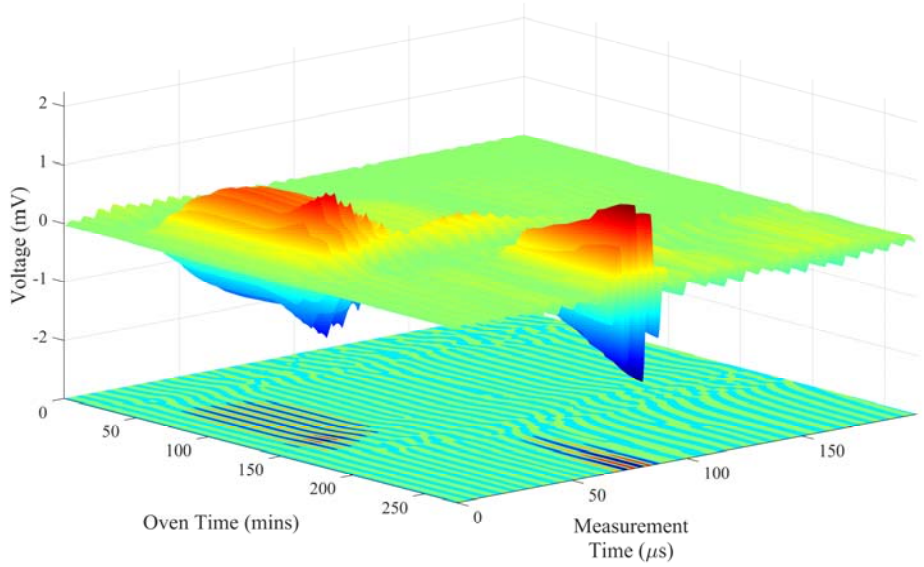

Figure 6. 3-D surface and contour plot of guided waves for 140 kHz actuation at sensor 4 throughout the cure.

Similar to Figure 6, the full time history of the plate response at sensor 4 excited by a five-cycle Hanning window toneburst actuation with a center frequency of 300 kHz is shown as a three-dimensional surface and contour plot in Figure 7.

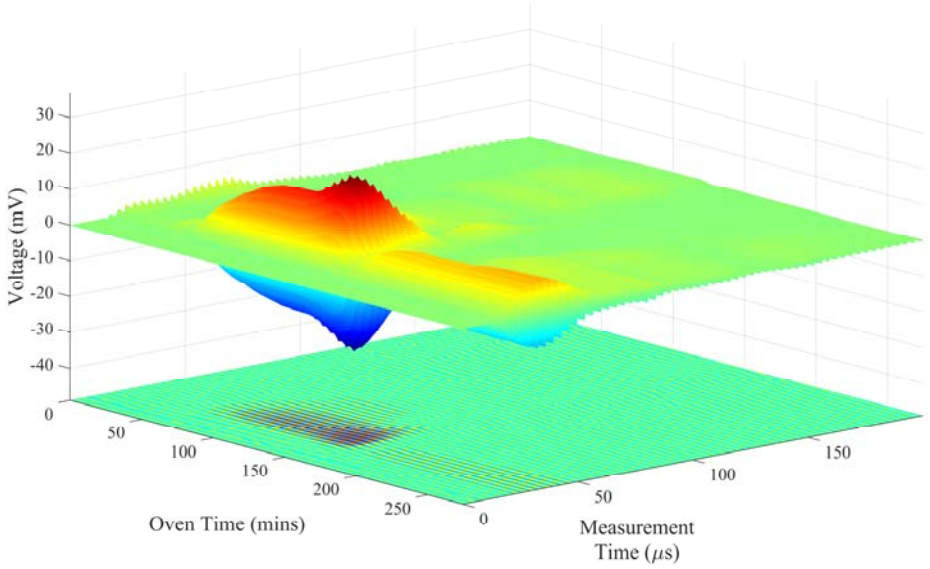

Figure 7. 3-D surface and contour plot of guided waves for 300 kHz actuation at sensor 4 throughout the cure.

In addition to the experimental study, a zero-dimensional (material only) simulation of the cure response (Figure 8) was performed using RAVEN® composite process simulation software. The material model utilized in RAVEN® is a semi-empirical material model [36] based on lab-scale tests (e.g., DSC and rheology) which were described in additional detail in the introduction section.

The average temperature of the two part thermocouples (Figure 3) was modeled as the temperature of the part. The degree of cure, cure rate, and resin viscosity were direct outputs of the simulation. For the thin part in this study, a zero-dimensional analysis was shown to have little difference in the composite curing response with a one-dimensional (drill-through) analysis. For the one-dimensional comparison analysis, the recorded air temperature of the oven and the average temperature of the two part thermocouples were utilized as inputs to the model. In this case, the two thermocouples taped to the outside of the vacuum bag using sealant tape (Figure 3) were modeled as the temperature of the vacuum bag. Heat transfer coefficients were applied at the boundaries of the model which included each material layer listed in the materials and methods section.

The glass transition temperature (T_g) was calculated using the DeBenedetto equation

$$T_g = T_{g0} + \frac{\lambda\sigma}{1-(1-\lambda)\sigma}\left(T_{g\infty} - T_{g0}\right) \tag{1}$$

where σ is the degree of cure and $\lambda = 0.78$, $T_{g0} = -7°C$, and $T_{g\infty} = 250°C$ which are model parameters for Hexcel® 8552 resin that are fit to experimental data during material characterization [36]. Vitrification occurs around the point at which the temperature of the composite resin becomes less than the glass transition or vitrification temperature [37] (Figure 8).

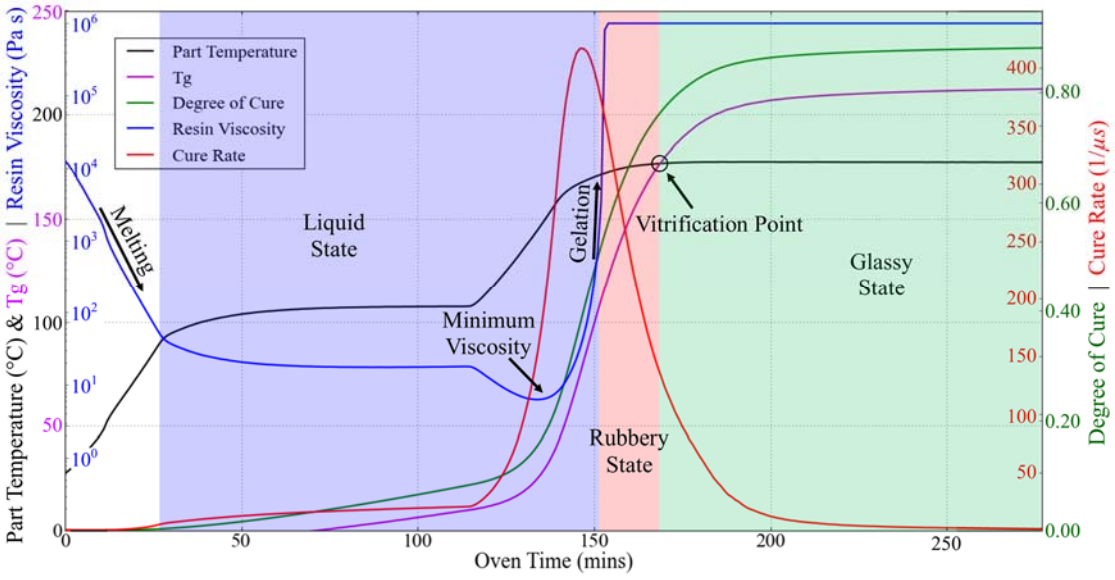

Figure 8. Cure response [part temperature (outside left axis), T_g (outside left axis), resin viscosity (inside left axis), degree of cure (outside right axis), cure rate (inside right axis), and vitrification point] as predicted by Hexcel 8552® material model [36] using RAVEN® composite process simulation software zero-dimensional analysis.

The Hilbert transform of a function, $f(t)$, defined as, $\tilde{f}(t)$, for all t is given by Eq. (2). From the Hilbert transform, the signal envelope, $A(t)$, in the time domain can be calculated by Eq. (3) [38].

$$\tilde{f}(t) = H(f(t)) = \frac{1}{\pi}\int_{-\infty}^{\infty}\frac{f(\tau)}{t-\tau}d\tau \tag{2}$$

where H denotes the Hilbert transform.

$$A(t) = \sqrt{f^2(t) + \tilde{f}^2(t)} \tag{3}$$

The peak voltage, V_{peak}, from every measurement was determined as the maximum of the signal envelope calculated by the Hilbert transform [Eq. (4)].

$$V_{peak}(OT_i, x_j, f_{c_k}) = \max_l(A(OT_i, x_j, f_{c_k}, t_l)) \tag{4}$$

where OT_i, x_j, and f_{c_k} denote the discrete oven time, location (i.e., sensor), and center frequency of actuation, respectively, at which the measurement was taken. For reference, the plate response in Figure 5 was taken at OT = 272 minutes, x = 114 mm (Sensor 4), and f_c = 140 kHz and the resulting peak voltage, V_{peak}, of the signal envelope was approximately 1.7 mV.

The peak voltages were then normalized by dividing the peak voltage value from every measurement by the maximum voltage observed during the entire cure cycle by that sensor and actuation frequency [Eq. (5)]. This normalized every peak voltage value to a number between zero and one.

$$V_{norm,peak}(OT_i, x_j, f_{c_k}) = \frac{V_{peak}(OT_i, x_j, f_{c_k})}{\max_i(V_{peak}(OT_i, x_j, f_{c_k}))} \tag{5}$$

All sensors measure the guided waves at an identical oven time in one measurement; however, since the system loops through the actuation center frequencies, measurements at different actuation center frequencies occur at slightly different oven times (approximately 30 s increments). Thus, $V_{norm,peak}$ was first interpolated at defined oven times. Then, $V_{norm,peak}$ was averaged across sensor and center actuation frequency at the defined oven times [Eq. (6)].

$$V_{avg,norm,peak}(OT) = \frac{1}{np}\sum_{k=1}^{p}\sum_{j=1}^{n}V_{norm,peak}(OT, x_j, f_{c_k}) \tag{6}$$

The average normalized peak voltages, $V_{avg,norm,peak}$, are the averaged results from every sensor and actuation frequency throughout the entire cure cycle. This was done to remove sensor and frequency variation in the results allowing for cleaner interpretation and communication of the effect of curing on the amplitude of the guided waves. It is expected that there is information of value in the frequency dependence of the results, which was outside the scope of this initial study. Figure 9 displays the air temperature and the average part thermocouple temperature recorded by the oven as well as the average normalized peak voltages of the guided waves throughout the cure cycle.

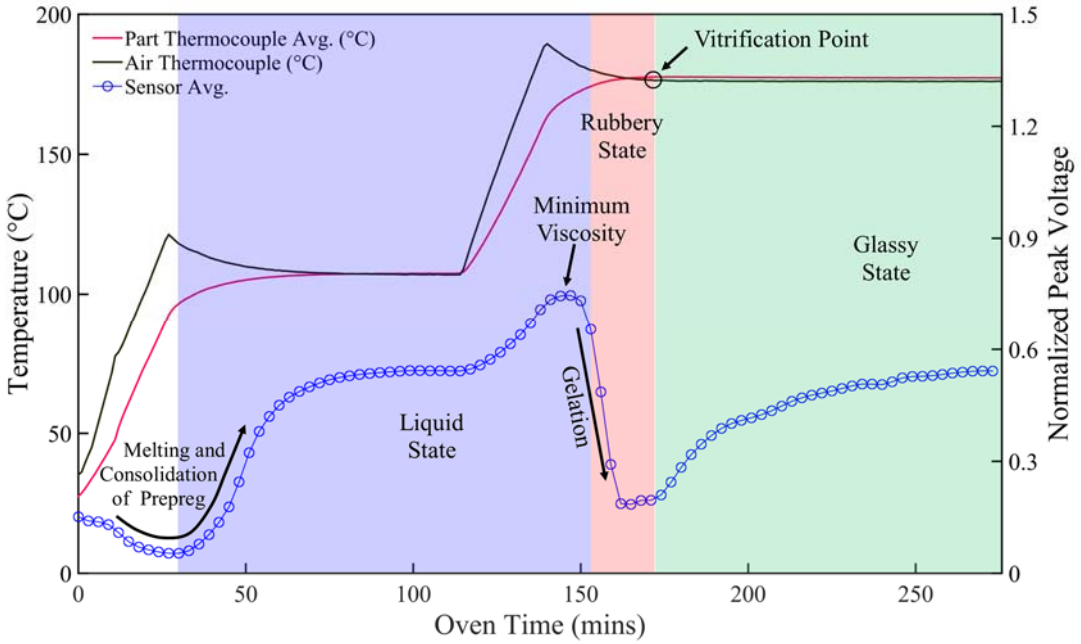

Figure 9. Normalized peak voltages of the guided waves averaged from each of the fourteen actuation frequencies and eight sensors measured throughout the cure cycle.

In Figure 10, the group velocity of the A_0 Lamb wave mode for five excitation frequencies (120, 130, 140, 150, 175, and 200 kHz) as well as the air temperature and the average part thermocouple temperature are shown. The A_0 Lamb wave mode was the dominant wave mode at these frequencies when the resin of the composite was in the glassy state, or in the transition from the rubbery to the glassy state (oven time approximately 175 to 270 minutes). This can be visualized more clearly in Figure 6. To determine the group velocity, the time of arrival (TOA), was identified by finding the measurement time at which V_{peak} occurred. A linear fit was then made to the sensor location, x, and TOA at each frequency and oven time. The slope of this fit is the group velocity, c_g [Eq. (7)].

$$x = c_g \times TOA + B \tag{7}$$

where B is a constant of the linear fit.

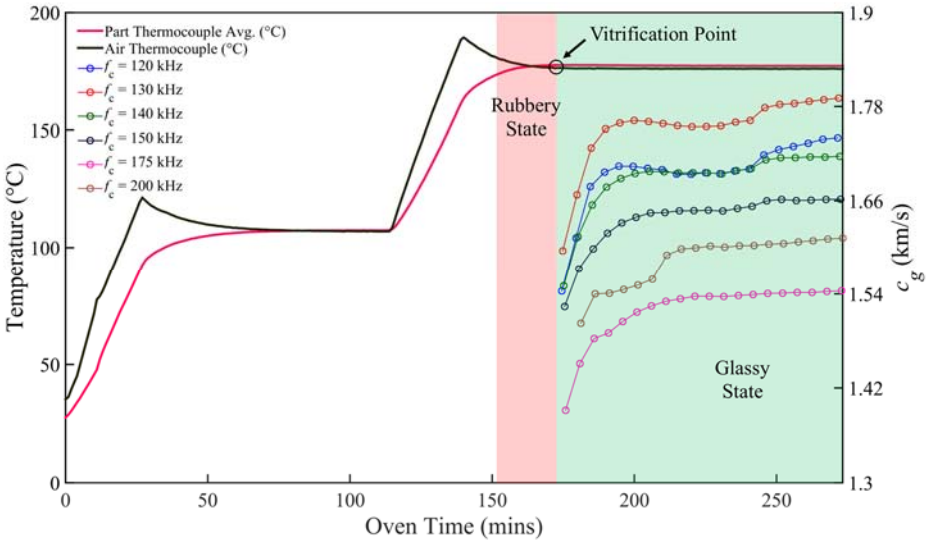

Figure 10. Group velocity of the A_0 wave mode for five excitation frequencies (120, 130, 140, 150, 175, and 200 kHz).

Figure 11 (a)-(d) are analogous to Figure 6 through Figure 9 for the modified cure cycle without the B-stage hold.

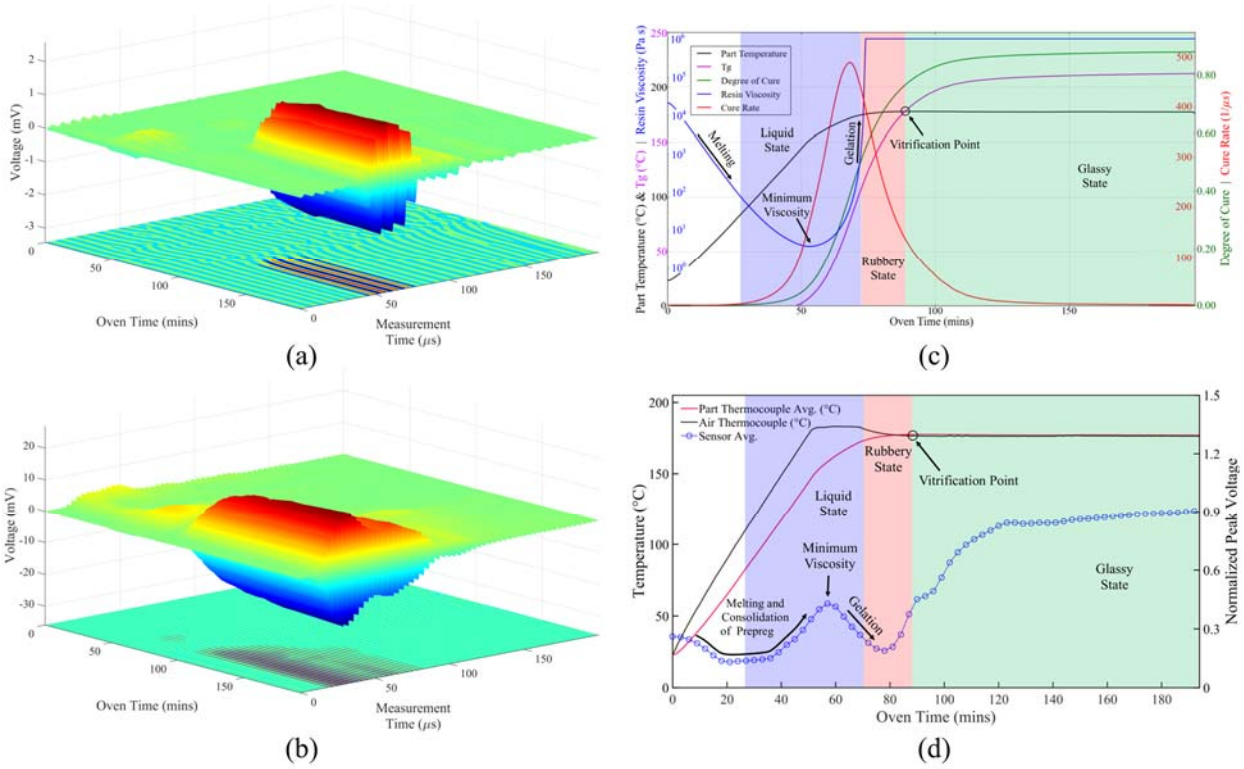

Figure 11. 3-D surface and contour plot of guided waves for (a) 140 kHz and (b) 300 kHz actuation at sensor 2 throughout cure, (c) cure response [part temperature (outside left axis), T_g (outside left axis), resin viscosity (inside left axis), degree of cure (outside right axis), cure rate

(inside right axis), and vitrification point] as predicted by Hexcel 8552® material model [36] using RAVEN®, and (d) average normalized peak voltages of the guided waves for the cure cycle without the B-stage hold.

4. Discussion

The key transition points during cure cycle can be identified from the newly developed cure monitoring system. First, as the resin melted and the composite started to consolidate, an increase in the normalized peak voltage of the guided waves was observed (Figure 9 and Figure 11d). During the ramp to 177°C, the viscosity dropped to a minimum and this corresponded to the maximum normalized peak voltage (Figure 9 and Figure 11d). When the resin began to gel, the normalized amplitude started dropping and continued to drop throughout gelation (Figure 9 and Figure 11d). This phenomenon is best understood by the analogy of dropping a pebble in a lake compared to honey. The wave created would have a higher amplitude (lower attenuation) in water than in the thicker, higher viscosity honey. Lastly, the normalized peak voltage increased throughout vitrification (transition from rubbery to glassy state) before nearing a plateau close to the end of cure (Figure 9 and Figure 11d). The time of vitrification was also consistent with previously published works on composites fabricated with Hexcel® 8552 resin [39-41]. These trends were observed in both cure cycles. An interesting difference between the two cure cycles was the ratio of the average normalized peak voltage when the resin was in the liquid state (including at minimum viscosity) compared with the glassy state near end of cure. The average normalized peak voltage was higher in the liquid state than the glassy stage for the two-stage cure cycle (Figure 9) when more cure time was spent in the liquid state. Whereas, the average normalized peak voltage was higher in the glassy state than in the liquid state for the cure cycle without the B-stage hold (Figure 11d). More investigation would be required to verify this trend as repeatable and understand its cause.

Next, as the degree of cure (Figure 8) from the Hexcel 8552® material model [36] simulated by RAVEN® increased, the group velocity (Figure 10) of the guided waves increased (i.e., degree of cure was directly proportional to group velocity). In addition, the group velocity curve resembled the upper half of the S-shape degree of cure curve. Although a quantitative equation for degree of cure based solely on group velocity was not presented in this work, the group velocity curve could be used as a qualitative measure to predict the degree of cure of the composite. Further investigation is needed to understand the frequency dependence of the group velocity. Each of these trends were consistent over the frequency range investigated when the A_0 wave mode was dominant. The A_0 wave mode became dominant near vitrification as the resin transitioned from the rubbery to glassy state. The development of the A_0 wave mode can be clearly seen in Figure 6 beginning at an oven time of approximately 175 minutes.

As mentioned previously, the goal of this work was not to produce a high quality composite panel but rather to develop and test the system and quality of the signals recorded during cure at elevated temperatures inside an oven. Additional modifications will be required to ensure the panels

fabricated have no sign of mark-off in the regions where the sensors were placed above the part on the caul.

Possible future research includes developing dispersion curves for the composite laminate during cure by understanding the wavenumber, phase velocity, and group velocity frequency dependence throughout the cure cycle. This will require denser spacing of the sensors to measure higher wavenumbers (smaller wavelengths) as with the A_0 wave mode. In addition, future work includes investigating the connection between the material, viscoelastic, and mechanical properties of the composite during cure with the group velocity and attenuation (Part two of Figure 2).

5. Conclusions

In summary, a preliminary automated cure monitoring system employing high-temperature piezoelectric transducers was developed to interrogate a twenty-four ply unidirectional composite panel fabricated from Hexcel® IM7/8552 prepreg during cure in an oven. The experimental guided wave results (identification of melting, minimum viscosity, gelation, and vitrification) correlate quite well with the simulation predictions of the semi-empirical material model which is based on data from experimental material characterization tests. The system and process initially developed in this work has the potential to be used in the future to dynamically control the cure cycle in a closed-loop process to maximize composite part quality and consistency. This is possible because the acquisition and analysis of the guided waves are done almost simultaneously in real-time during cure. The guided wave system is incorporated directly into standard curing equipment and technique and could be scaled from producing flat composite panels, as in this work, to full-scale complex structures (e.g., cylinders/barrels, wing skins, etc.). Using guided waves throughout the entire cure cycle (i.e., in-situ measurements during liquid, rubbery, and glassy states) pushes the technology envelope forward as guided waves are typically applied to solid medium. To the authors' knowledge, this is the first application of measuring guided waves in composites (or any other material system) as they are propagating in the part during cure.

6. Acknowledgements

The work is performed in the Advanced Materials and Processing Branch at NASA Langley Research Center. The authors would like to acknowledge the financial support from a Graduate Research Assistantship at National Institute of Aerospace through the Advanced Composites Project (ACP) at NASA Langley Research Center.

7. References

1. Hou, T. H. 2014. "Cure cycle design methodology for fabricating reactive resin matrix fiber reinforced composites: A protocol for producing void-free quality laminates," *NASA TM 2014-218524*: 1-16.

2. Birt, E. and R. Smith. 2004. "A review of NDE methods for porosity measurement in fibre-reinforced polymer composites," *Insight-Non-Destructive Testing and Condition Monitoring*, 46: 681-686.

3. J.M. Barton. 1985. "The application of differential scanning calorimetry (DSC) to the study of epoxy resin curing reactions," in: K. Dusek (Ed.), *Epoxy Resins and Composites I*, Springer, pp. 111-154.

4. Fava, R. 1968. "Differential scanning calorimetry of epoxy resins," *Polymer*, 9: 137-151.

5. Prime, R. B. 1973. "Differential scanning calorimetry of the epoxy cure reaction," *Polymer Engineering & Science*, 13: 365-371.

6. Vyazovkin, S. and N. Sbirrazzuoli. 1996. "Mechanism and kinetics of epoxy-amine cure studied by differential scanning calorimetry," *Macromolecules*, 29: 1867-1873.

7. Hardis, R., J. L. Jessop, F. E. Peters, and M. R. Kessler. 2013. "Cure kinetics characterization and monitoring of an epoxy resin using DSC, Raman spectroscopy, and DEA," *Composites Part A: Applied Science and Manufacturing*, 49: 100-108.

8. De Bruyne, N. 1956. "The adhesive properties of epoxy resins," *Journal of Applied Chemistry*, 6: 303-310.

9. Kaelble, D. 1965. "Dynamic and tensile properties of epoxy resins," *Journal of Applied Polymer Science*, 9: 1213-1225.

10. Hou, T. H., J. Y. Huang, and J. A. Hinkley. 1990. "Chemorheology of an epoxy resin system under isothermal curing," *Journal of Applied Polymer Science*, 41: 819-834.

11. Meyers, M. A. and K. K. Chawla. 2009. *Mechanical behavior of materials*. Cambridge University Press.

12. McIlhagger, A., D. Brown, and B. Hill. 2000. "The development of a dielectric system for the on-line cure monitoring of the resin transfer moulding process," *Composites Part A: Applied Science and Manufacturing*, 31: 1373-1381.

13. Coats, A. and J. Redfern. 1963. "Thermogravimetric analysis. A review," *Analyst*, 88: 906-924.

14. Nixdorf, K. and G. Busse. 2001. "The dielectric properties of glass-fibre-reinforced epoxy resin during polymerisation," *Composites Science and Technology*, 61: 889-894.

15. Compton, D. A., S. L. Hill, N. A. Wright, M. A. Druy, J. Piche, W. A. Stevenson, and D. W. Vidrine. 1988. "In situ FT-IR analysis of a composite curing reaction using a mid-infrared transmitting optical fiber," *Applied Spectroscopy*, 42: 972-979.

16. George, G., P. Cole-Clarke, N. St John, and G. Friend. 1991. "Real-time monitoring of the cure reaction of a TGDDM/DDS epoxy resin using fiber optic FT-IR," *Journal of Applied Polymer Science*, 42: 643-657.

17. Aust, J. F., J. B. Cooper, K. L. Wise, and B. J. Jensen. 1999. "In situ analysis of a high-temperature cure reaction in real time using modulated fiber-optic FT-Raman spectroscopy," *Applied Spectroscopy*, 53: 682-686.

18. Cooper, J. B., K. L. Wise, and B. J. Jensen. 1997. "Modulated FT-Raman fiber-optic spectroscopy: A technique for remotely monitoring high-temperature reactions in real-time," *Analytical Chemistry*, 69: 1973-1978.

19. Musto, P., M. Abbate, G. Ragosta, and G. Scarinzi. 2007. "A study by Raman, near-infrared and dynamic-mechanical spectroscopies on the curing behaviour, molecular structure and viscoelastic properties of epoxy/anhydride networks," *Polymer*, 48: 3703-3716.

20. Lindrose, A. M. 1978. "Ultrasonic wave and moduli changes in a curing epoxy resin," *Experimental Mechanics*, 18: 227-232.

21. Speake, J., R. Arridge, and G. Curtis. 1974. "Measurement of the cure of resins by ultrasonic techniques," *Journal of Physics D: Applied Physics*, 7: 412.

22. Adams, R. and P. Cawley. 1988. "A review of defect types and nondestructive testing techniques for composites and bonded joints," *NDT International*, 21: 208-222.

23. Chen, J., S. Hoa, C. Jen, and H. Wang. 1999. "Fiber-optic and ultrasonic measurements for in-situ cure monitoring of graphite/epoxy composites," *Journal of Composite Materials*, 33: 1860-1881.

24. Maffezzoli, A., E. Quarta, V. Luprano, G. Montagna, and L. Nicolais. 1999. "Cure monitoring of epoxy matrices for composites by ultrasonic wave propagation," *Journal of Applied Polymer Science*, 73: 1969-1977.

25. Lionetto, F., A. Tarzia, and A. Maffezzoli. 2007. "Air-coupled ultrasound: a novel technique for monitoring the curing of thermosetting matrices," *IEEE Transactions on Ultrasonics, Ferroelectrics and Frequency Control*, 54: 1437-1444.

26. Liebers, N., F. Raddatz, and F. Schadow. 2013. *Effective and flexible ultrasound sensors for cure monitoring for industrial composite production.* Deutsche Gesellschaft für Luft-und Raumfahrt-Lilienthal-Oberth eV.

27. Stone, D. and B. Clarke. 1975. "Ultrasonic attenuation as a measure of void content in carbon-fibre reinforced plastics," *Non-destructive Testing*, 8: 137-145.

28. Jeong, H. and D. Hsu. 1995. "Experimental analysis of porosity-induced ultrasonic attenuation and velocity change in carbon composites," *Ultrasonics*, 33: 195-203.

29. Pavlopoulou, S., C. Soutis, and W. Staszewski. 2012. "Cure monitoring through time-frequency analysis of guided ultrasonic waves," *Plastics, Rubber and Composites*, 41: 4-5.

30. Hudson T. B., B. W. Grimsley, and F. G. Yuan. 2016. "Development of a fully automated guided wave system for in-process cure monitoring of CFRP composite laminates," Proceedings of the American Society for Composites: Thirty-First Technical Conference, September 19-21, 2016.

31. Hudson T. B., T. H. Hou, B. W. Grimsley, and F. G. Yuan. 2015. "Detection of CFRP composite manufacturing defects using a guided wave approach," Proceedings SAMPE Technical Conference, May 18-May 21, 2015.

32. Farquharson S., J. Carignan, V. Khitrov, A. Senador, and M. Shaw. 2004. "Development of a phase diagram to control composite manufacturing using Raman spectroscopy," Proceedings SPIE 5272, Industrial and Highway Sensors Technology, March 8, 2004.

33. Gillham J. K. 1987. "Formation and properties of thermosetting and high Tg polymeric materials," Makromolekulare Chemie. Macromolecular Symposia.

34. Farquharson S., J. Carignan, V. Khitrov, A. Senador, and M. Shaw. 2004. "Development of a phase diagram to control composite manufacturing using Raman spectroscopy," Optical Technologies for Industrial, Environmental, and Biological Sensing.

35. M.T. Aronhime, J.K. Gillham. 1986. "Time-temperature-transformation (TTT) cure diagram of thermosetting polymeric systems," in: K. Dusek (Ed.), *Epoxy Resins and Composites III*, Springer, pp. 83-113.

36. Ee, D. V. and A. Poursartip. 2009. "HexPly 8552 material properties database for use with COMPRO CCA and RAVEN," National Center for Advanced Materials Performance.

37. Paul, D. R. and Y. P. Yampol'skii. 1993. *Polymeric gas separation membranes.* CRC press.

38. Johansson, M. 1999. "The hilbert transform," *Mathematics Master's Thesis.Växjö University, Suecia.Disponible en internet: http://w3.msi.vxu.se/exarb/mj_ex.pdf, consultado el*, 19.

39. Ersoy, N., K. Potter, M. R. Wisnom, and M. J. Clegg. 2005. "An experimental method to study the frictional processes during composites manufacturing," *Composites Part A: Applied Science and Manufacturing*, 36: 1536-1544.

40. Ersoy, N., K. Potter, M. R. Wisnom, and M. J. Clegg. 2005. "Development of spring-in angle during cure of a thermosetting composite," *Composites Part A: Applied Science and Manufacturing*, 36: 1700-1706.

41. Ersoy, N., T. Garstka, K. Potter, M. R. Wisnom, D. Porter, M. Clegg, and G. Stringer. 2010. "Development of the properties of a carbon fibre reinforced thermosetting composite through cure," *Composites Part A: Applied Science and Manufacturing*, 41: 401-409.